On the Performance of Acousto Optical Modulators–Free Space Optical Wireless Communication Systems over Negative Exponential Turbulent Channel

Raed Mesleh(✉), Ayat Olaimat, and Ala Khalifeh

Department of Electrical and Communication Engineering,
School of Electrical Engineering and Information Technology,
German Jordanian University, Amman, Jordan
raed.mesleh@gju.edu.jo

Abstract. A novel free space optical (FSO) wireless communication system is proposed very recently utilizing acousto optical modulator (AOM) to externally modulate the laser beam [1]. The idea is to control the diffracted angle of a laser beam incident to an AOM through varying the acoustic frequency propagating inside the AOM. The receiver with multiple photo diodes, spatially distributed and aligned to the preplanned diffracted angles, receive the laser signal and retrieve the transmitted bits. In this paper, we study the performance of AOM–FSO system over negative exponential turbulent channel. A closed-form expression for the average bit error probability is derived and shown to be precise over wide range of channel and system parameters. The performance of the system is compared to the ideal case of no fading and log normal channel.

Keywords: Acousto Optical Modulator (AOM)
Free Space Optics (FSO) · Performance analysis
Wireless communication · Negative exponential channel

1 Introduction

Optical wireless communication (OWC) is an auspicious technology for next generation wireless communication systems due to its multiple inherent advantages. OWC utilizes a huge unlicensed spectrum and predicts a vast increase in the spectral efficiency [2,3]. Free space optical (FSO) is the outdoor technology part of OW communication systems. The market of FSO is expected to grow by 41.4% between 2017 and 2022, according to a recent *Markets and Markets* technical report. Such increase is driven mainly by: *(i)* free and unregulated licensing, *(ii)* enhanced energy efficiency, *(iii)* low carbon emission, and *(iv)* no interference with RF signals.

V. Sucasas et al. (Eds.): BROADNETS 2018, LNICST 263, pp. 307–316, 2019.
https://doi.org/10.1007/978-3-030-05195-2_30

Modulating the intensity of the propagating light is not trivial as the transmitted light has to be positive and real signal [4]. At the receiver, direct detection is generally considered where the variant intensities of the received light are directly converted to current signal. However, weather conditions and scattering severely degrade the performance of FSO system. In particular, weather conditions, such as fog, cause absorption and scattering, which severely degrades the performance [5]. Other issues include deviation of the laser beam, misalignment and angular alterations [6,7]. In particular, misalignment in the link will importantly affect the link performance [8,9].

A novel idea reported recently, called *Acousto optical modulator–FSO (AOM–FSO)*, demonstrated significant performance enhancements over log-normal fading channels [1]. AOM is a device that operates by Bragg diffraction of an incident light beam from an input acoustic signal. The diffracted light intensity and other parameters are controlled through the parameters of the incident acoustic wave. Also, the parameters of the acoustic signal depend on the frequency of the RF signal at the input of the piezoelectric driver at the input of the Bragg cell. For the AOM to function properly, proper design and several conditions must be met simultaneously [1,10,12–14].

In AOM-FSO system, incoming data bits frequency modulate an RF signal, which determines the acoustic wave signal parameters at the output of a piezoelectric transducer [10]. An incident and un-modulated laser beam signal will be diffracted with a frequency that is either decreased or increased by an amount proportional to the acoustic frequency. As such, varying the parameters of the incident acoustic signal control the parameters of the diffracted light beam. In [1], incoming data bits control the resulting acoustic frequency and determine the diffraction angle of the incident laser beam. The receiver considers multiple photo diodes (PD) aligned to the diffracted angles to estimate the modulated angle and retrieve original information bits.

The performance of AOM–FSO system has been analyzed over log–normal channels only in [1]. In this paper, we analyze and discuss the performance of AOM-FSO system over negative exponential (NE) turbulent channel. An accurate formula for the average bit error rate (BER) performance is derived and shown to be accurate over wide range of parameters. Monte Carlo simulation results are presented and discussed to highlight the accuracy of the derived formulas and to study the impact of different channel parameters on the performance.

The remaining of this article is ordered as follows. A revised system model is presented in Sect. 2 along with the considered channel model. Analytical derivation of the average BER is conducted in Sect. 3. Discussion and illustrative results are presented in Sect. 4 and conclusions are drawn in Sect. 5.

2 System and Channel Models

2.1 AOM-FSO System Model

In AOM-FSO system, incoming data bits enter a frequency shift keying (FSK) modulator that is connected to a piezoelectric transducer at the input of the

AOM. In particular, each m bits modulate a specific carrier frequency, f_{i}, $i = 1, 2, \cdots, M$, with $M = 2^m$ being the number of modulated RF signals. The generated RF frequencies control the piezoelectric transducer output acoustic frequency and an acoustic wave with velocity v_s and $\Lambda = v_s/f_s$ wavelength, propagates through the Bragg cell [11]. AOM-FSO system assumes that an unmodulated laser beam with λ_0 wavelength and P_i power hits the Bragg cell at the Bragg angle, θ_B. The incident optical beam and the acoustic wave interacts and is the cause behind the term *acousto optical modulator (AOM)*. Entering the laser beam at the Bragg angle guarantees the maximum diffraction of the laser beam as given by [11, p. 805, (20.0-1)]

$$\sin(\theta_B) = \frac{\lambda_0}{2n\Lambda}. \tag{1}$$

It is important to note that there exist a unique Bragg angle for each Λ assuming fixed λ_0. Hence, [1] proposes a small changes in the acoustic frequency leading to variant diffraction angles of the incident laser beam around the Bragg angle. Considering a propagating acoustic inside the Bragg cell with v_s velocity, f_s frequency and $q = \frac{2\pi}{\Lambda}$ wave number, results in an acoustic wave intensity given as [11, p. 802, (20.1-2)]

$$I_s = 0.5\varphi v_s^3 S_0, \ \left(W/m^2\right), \tag{2}$$

with φ being the medium mass density in $\left(Kg/m^3\right)$ and S_0 denoting the strain amplitude. The variation of the refractive index due to the presence of an acoustic wave is calculated as [11, p. 803, (20.1-6)]

$$\Delta n = \left(0.5\mathcal{M}I_s\right)^{1/2}, \tag{3}$$

where Δn denotes the changes in the refractive index and $\mathcal{M}$ is a parameter capturing the effectiveness of varying the refractive index of the medium through the acoustic wave.

The AOM-FSO leads to diffracted laser beam by an angle θ_r and optical power P_r given as [11, p. 803, (20.1-6)]

$$P_r = 2\pi^2 n_0^2 \frac{L^2\Lambda^2}{\lambda_0^4}\mathcal{M}I_s P_i, \tag{4}$$

with acoustic cell length being L and the refractive index of the medium in the absence of acoustic wave is n_0. The idea of AOM-FSO is to place M receiver PDs at d distance from the Bragg cell. The considered PDs should have a peak responsivity matching the reflected beam frequency. Each considered PD should be properly aligned to one of the pre-designed diffracted angles. Hence, the power at the input of the PD is written as

$$P_{\mathrm{rx}} = \frac{A_{\mathrm{rx}} T 10^{-\alpha\frac{d}{10}} P_r}{\pi(0.5\delta_\theta d)^2} + P_g, \tag{5}$$

where the area of the PD is denoted by $A_{\text{rx}} = \pi(0.5D)^2$, the overall optical efficiency is T, the laser beam-divergence is given by δ_θ and the undesired environment dependent background noise is P_g. The idea behind AOM–FSO system is to let the incoming m bits to modulate frequency signal that will results in unique acoustic signal. Accordingly, each sequence of bits will diffract the laser beam by a certain diffraction angle, θ_i, $i = 1, 2, \cdots, M$. Having M PDs with d_r spacing each properly aligned to one angle facilitate the receiver detection process.

At the output of the Bragg cell, the light is propagated in free space and the signal at the input of the the i^{th} PD is given by

$$P_{r_i} = \eta\beta P_{\text{rx}}^i h_i + n_i, \quad i = 1, 2, \cdots, M, \tag{6}$$

with η being conversion efficiency, h_i is the channel irradiance between the i^{th} receiver and the Bragg cell and the thermal noise and the shot noise radiations are denoted by n_i which is assumed to white Gaussian process with zero mean and σ_n^2 variance. The normalized path-loss term, β, is

$$\beta = \frac{\beta_k}{\beta_{d_i}(d)}, \tag{7}$$

where $\beta_{d_i}(d)$ is the path loss in clear weather conditions and β_k is the path loss in the presence of weather attenuations given by [5]

$$\beta_k = \frac{D_R 10^{\frac{-\alpha d}{10}}}{(D_T + \delta_\theta d)^2}, \tag{8}$$

where D_R being the PD diameter, D_T the transmitting laser diameter and α denotes the weather-dependent attenuation coefficient (in dB/km), obtained as [5]

$$\alpha = \frac{3.91}{v}\left(\frac{\lambda}{550\,(nm)}\right)^P, \tag{9}$$

with v being the visibility parameter and P is the size distribution coefficient of scattering, which can be obtained according to Kim model as [16]

$$P = \begin{cases} 1.6 & v > 50 \\ 1.3 & 6 < v < 50 \\ 0.16v + 0.34 & 1 < v < 6 \\ v - 0.5 & 0.5 < v < 1 \\ 0 & v < 0.5 \end{cases}. \tag{10}$$

The normalized path loss values at different weather conditions are tabulated in Table 1. To estimate the diffracted angle of the laser been, the following formula is considered [1]

$$\hat{\theta}_r = \arg \max_{i \in \{1:M\}} (\mathbf{r}), \tag{11}$$

Table 1. Normalized path loss values at different weather conditions and at $\lambda = 690$ nm.

Weather condition	Visibility	Path loss (dB/Km)	Normalized path loss (β)
Clear	19	1.58	0.98
Thin fog/Heavy rain	1.9	7.72	0.1939
Moderate fog	0.5	33.96	0.00046
Thick fog	0.2	84.9	0.000000003712

where $\mathbf{r} = \left[r_1 \; r_2 \cdots r_m \right]^T$ contains all possible received signal powers at each instant of transmission time. The source bits, which results in the estimated diffracted angle can be retrieved by inverse mapping process.

The received signal to noise ratio (SNR) is given by

$$\bar{\gamma} = \frac{\eta P_{\text{rx}}}{\sigma_n^2}. \tag{12}$$

2.2 Negative Exponential Channel (NE)

The probability distribution function (PDF) of the NE channel is given by

$$f_h\left(h_i\right) = \frac{1}{h_i} \exp\left(-h_i\right), \tag{13}$$

and the PDF of the instantaneous SNR at the i^{th} PD is

$$f_\gamma\left(\gamma\right) = \frac{1}{2\sqrt{\gamma\bar{\gamma}}} \exp\left(\sqrt{\frac{\bar{\gamma}}{\gamma}}\right). \tag{14}$$

3 Performance Analysis

In what follows, the average BER of AOM-FSO system is derived over NE fading channel and in the presence of atmospheric attenuations. The derivation follows similar procedure as proposed in [1] and using the receiver presented in previous section. Initially, the special case of $M = 2$ is assumed and then generalized for arbitrary values of M. Considering (11) and $M = 2$, the BER can be written as

$$P_b = \Pr\left[r_2 > r_1 \,|\theta_1\right]. \tag{15}$$

(15) states that an error occurs if the received power at the second PD, r_2, was larger than the received power at the first PD, r_1, given that the input bits modulate θ_1. Hence, the detection process is obtained by finding the index of PD the received the maximum power among all received signals, $\mathbf{r} = \left[r_1 \; r_2 \cdots r_M \right]^T$, with $(\cdot)^T$ being the vector/matrix transpose operation. Analytically, this is the

same as computing the PDFs of a sorted M random variables each with a unique mean value. This can be roughly estimated as an order statistics formula [15].

Let the order statistics of a random continuous population sample be $X_1, X_2, \cdots, X_M$ with $X_M > X_{(M-1)} > \cdots > X_1$, each with a cumulative distribution function (CDF) $F_X\left(x\left|\mu_x, \sigma_x^2\right.\right)$ and a PDF of $f_X\left(x\left|\mu_x, \sigma_x^2\right.\right)$. Thereby, the PDF of X_i is

$$f_{x_i}(x\left|\mu_i, \sigma_x^2\right.) = \frac{M!}{(i-1)!\,(M-i)!}\left[F_X\left(x\left|\mu_x, \sigma_x^2\right.\right)\right]^{i-1} \times\left[1 - F_X\left(x\left|\mu_x, \sigma_x^2\right.\right)\right]^{M-i} f_X\left(x\left|\mu_x, \sigma_x^2\right.\right). \tag{16}$$

For the considered AOM-FSO system over NE channel and in the presence of AWGN, the PDF of the ordered random variables is

$$f_\gamma\left(X\right|\mu_h, \sigma_h^2) = \frac{1}{2\sqrt{\gamma\bar{\gamma}}} \exp\left(\sqrt{\frac{\bar{\gamma}}{\gamma}}\right) \times \frac{1}{2}\left(1 + \exp\left(\sqrt{\frac{\bar{\gamma}}{\gamma}}\right)\right). \tag{17}$$

Assuming $M = 2$, the error probability is calculated as

$$P_b = \frac{1}{M}\left(\Pr\left[f_{r_1}\left(\gamma\left|\mu_h, \sigma_h^2\right.\right) < f_{r_2}\left(\gamma\left|\mu_h, \sigma_h^2\right.\right)|\theta_1\right] + \Pr\left[f_{r_2}\left(\gamma\left|\mu_h, \sigma_h^2\right.\right) < f_{r_1}\left(\gamma\left|\mu_h, \sigma_h^2\right.\right)|\theta_2\right]\right). \tag{18}$$

The probability of error in (18) can be computed as

$$P_b = \frac{1}{M}\left\{\int_0^{\varepsilon_1} f_{r_1}\left(\gamma\left|\mu_h, \sigma_h^2\right.\right) d\gamma + \int_0^{\varepsilon_2} f_{r_2}\left(\gamma\left|\mu_h, \sigma_h^2\right.\right) d\gamma\right\}, \tag{19}$$

where ε_1 indicates the intersection point between the two PDFs, which are computed numerically.

A list of intersection points for different values of d and d_r are respectively provided in Tables 2 and 3.

For arbitrary values of M, the BER can be calculated as

$$P_b = \frac{1}{M}\sum_{i=1}^{M}\int_0^{\varepsilon_i} f_{r_i}\left(\gamma\left|\mu_h, \sigma_h^2\right.\right) d\gamma. \tag{20}$$

Table 2. Intersection points for different values of d assuming $d_r = 1.25$ cm over NE turbulent channels.

d (Km)	ε for $M = 2$	ε for $M = 4$
1.1	5.8	5.5
2	3.3	3.3
2.5	5	5

Table 3. Intersection points for different values of d_r cm assuming $d = 1$ Km over NE turbulent channels.

d_r (cm)	ε for $M = 2$	ε for $M = 4$
1	3.5	3.5
1.75	7.5	6.4

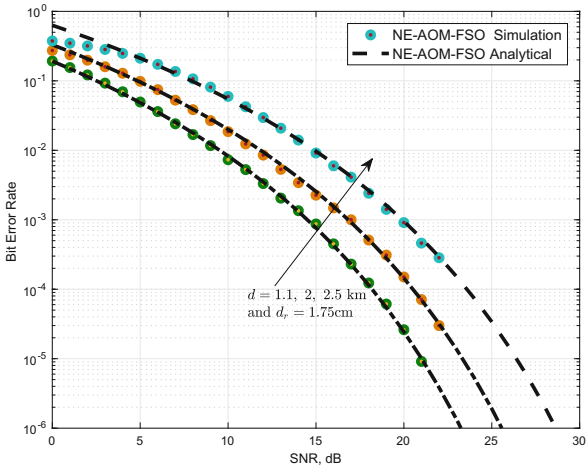

Fig. 1. Analytical and simulation BER results of AOM-FSO system over NE channel for different values of d and $M = 2$.

4 Results

The considered simulation parameters in this paper are listed in Table 4. Also, the pre-designed diffraction angles along with the corresponding acoustic frequencies and the amount of diffracted power are tabulated in Table 5.

Table 4. Simulation Parameters

Laser parameters		Acoustic parameters	
λ_0	1318 nm	L	25.4×10^{-3} m
P_i	10 dB	v_s	3.63×10^{-3} m/s
δ_θ	3.5×10^{-5} rad	$\mathcal{M}$	1.67×10^{-14} m^2/W
θ_B	0.0213 rad	I_s	35 W/m^2
T	1	A_{rx}	4.9×10^{-4} m^2

Table 5. Diffraction angles, powers and acoustic frequencies assuming $P_i = 10$ W.

Acoustic frequency f_s	Diffraction angles θ_r	Diffracted power P_r
224.09 MHz	0.0213 rad	9.9925 W
224.35 MHz	0.021325	9.9915 W
224.622 MHz	0.02135	9.9904 W
224.88 MHz	0.021375	9.9892 W

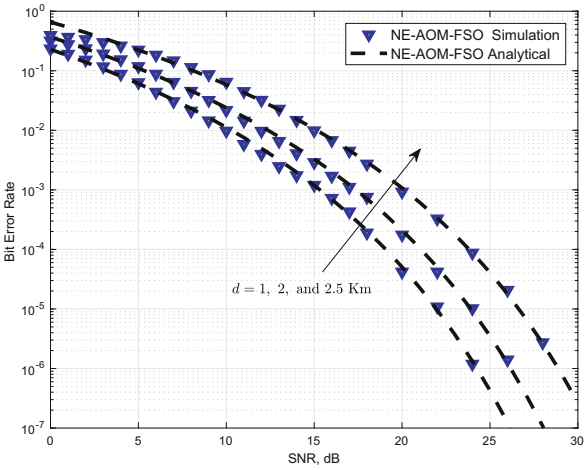

Fig. 2. Analytical and simulation BER results of AOM-FSO system over NE channel for different values of d and $M = 4$.

In the first results depicted in Fig. 1, analytical and simulation BER results for AOM-FSO system over NE channel assuming $\sigma_h = 0.1$, $d_r = 1.75$ cm, $M = 2$ and different values of d are illustrated. Increasing d is shown to deteriorate the performance. This degradation is not due to higher path losses at higher distances, since SNR values are assumed to be the same. The error is rather due to the increase in beam divergence at higher distances, which results in higher BER values. Similar results are reported in Fig. 2 but for $M = 4$. Similar conclusion as made on the previous figure can be stated here as well.

A comparison between the performance of AOM-FSO system over log normal and NE channels is studied and results are shown in Fig. 3. NE channels model high turbulent distribution and degrades the performance of AOM-FSO system as compared to log normal channels. Besides, the lower visibility weather conditions is shown to degrade the performance where the presence of thin-fog is shown to degrade the performance by about 13 dB.

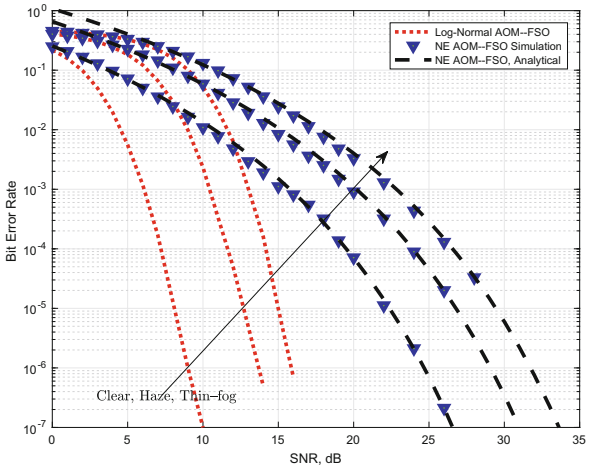

Fig. 3. AOM-FSO performance comparison results over log normal and NE channels in the presence of different weather conditions assuming $d = 1$ Km, $d_r = 1.25$ cm, $\sigma_h = 0.1$ and $M = 4$.

5 Conclusions

This paper studies and analyzes the performance of the recently proposed AOM-FSO system over NE fading channels. Reported results validate the accuracy of the conducted analysis for a wide range of system and channel parameters. The impact of variant weather conditions is also studied and lack of visibility is shown to severely degrade the performance.

Acknowledgment. The work in this paper was supported from the Scientific Research Foundation at the Ministry of Higher Education in Amman, Jordan under grant number ICT/1/9/2016.

References

1. Mesleh, R., Al-Oleimat, A.: Acousto-optical modulators for free space optical wireless communication systems. J. Opt. Commun. Netw. **10**(5), 515–522 (2018)
2. Ghassemlooy, Z., Popoola, W., Rajbhandari, S.: Optical Wireless Communications: System and Channel Modelling with MATLAB. CRC Press, Boca Raton (2017)
3. CISCO, Cisco visual networking index: Global mobile data traffic forecast update, 2015–2020. CISCO, White paper, February 2016
4. Elgala, H., Mesleh, R., Haas, H.: Indoor optical wireless communication: potential and state-of-the-art. IEEE Commun. Mag. **49**(9), 56–62 (2011). ISSN 0163–6804
5. Abaza, M., Mesleh, R., Mansour, A., el Hadi Aggoune: Performance analysis of miso multi-hop FSO links over log-normal channels with fog and beam divergence attenuations. Optics Commun. **334**, 247–252 (2015). http://www.sciencedirect.com/science/article/pii/S0030401814008116

6. Lee, E.J., Chan, V.W.S.: Part 1: optical communication over the clear turbulent atmospheric channel using diversity. IEEE J. Sel. Areas Commun. **22**(9), 1896–1906 (2004)
7. Arnon, S.: Effects of atmospheric turbulence and building sway on optical wireless-communication systems. Opt. Lett. **28**, 129–131 (2003)
8. Khalighi, M.A., Uysal, M.: Survey on free space optical communication: a communication theory perspective. IEEE Commun. Surv. Tutor. **16**(4), 2231–2258 (2014)
9. Khalighi, M.-A., Schwartz, N., Aitamer, N., Bourennane, S.: Fading reduction by aperture averaging and spatial diversity in optical wireless systems. J. Opt. Commun. Netw. **1**(6), 580–593 (2009)
10. Chang, I.C.: Acousto optic devices and applications. IEEE Trans. Sonics Ultrason. **23**(1), 2–21 (1976)
11. Saleh, B.E.A., Teich, M.C.: Fundamentals of Photonics. Wiley, New York (1991). chapter 12
12. Eghbal, M., Abouei, J.: Security enhancement in free-space optics using acousto-optic deflectors. IEEE/OSA J. Opt. Commun. Netw. **6**(8), 684–694 (2014)
13. Nikulin, V.V., Khandekar, R., Sofka, J., Tartakovsky, G.: Acousto-optic pointing and tracking systems for free-space laser communications. In: Proceedings of SPIE, vol. 5892, no. 589216, August 2005
14. Ghosh, A.K., Verma, P., Cheng, S., Huck, R.C., Chatterjee, M.R., Al-Saedi, M.: Design of acousto-optic chaos based secure free-space optical communication links. In: Proceedings of SPIE, vol. 7464, no. 74640l (2009)
15. Casella, G., Berger, R.L.: Statistical Inference, 2nd edn. Duxbury, Pacific Grove (2002)
16. Kadhim, et al.: Characterization study and simulation of MIMO FSO communication under different atmospheric channel. Int. J. Innov. Sci. Eng. Technol. **3**(8) (2016). ISSN (Online) 2348 – 7968